Nesma Baa Belmessaoud, Naima Bouslah* and Nabila Haddadine

Clay/(PEG-CMC) biocomposites as a novel delivery system for ibuprofen

https://doi.org/10.1515/polyeng-2019-0390 Received December 26, 2019; accepted February 22, 2020; previously published online April 1, 2020

Abstract: In this study we report on the preparation and characterization of biocomposites based on a sodium montmorillonite-ibuprofen (MtIb) hybrid and neat poly(ethylene glycol), neat sodium carboxymethylcellulose or poly(ethylene glycol)-carboxymethylcellulose blend 50/50 biocomposites as drug carriers. Ib, a poorly soluble drug, was first intercalated into sodium Mt and then the resulting hybrid was compounded with the different polymeric matrices. Ib incorporation efficiency in Mt was determined by UV-visible spectroscopy, Fourier transform infrared spectroscopy, X-ray diffraction and thermal analysis. Both X-ray diffraction and differential scanning calorimetric studies revealed that the intercalation of Ib between the clay layers induced amorphization of the drug. Differential scanning calorimetry and Fourier transform infrared spectroscopy revealed the development of strong interactions between Ib and the polymer matrix. A study of the release of Ib from the synthesized biocomposites in simulated intestinal fluid (pH 7.4) was investigated. To better understand the release mechanism of drug molecules from the different carriers, several kinetic models have been applied.

Keywords: biocomposites; drug delivery; montmorillonite; polymer blends; specific interactions.

1 Introduction

In the last decades, there has been growing interest in the development of drug delivery systems between clay minerals and biopolymers for controlled drug delivery

*Corresponding author: Naima Bouslah, USTHB, Laboratoire de Synthèse Macromoléculaire et Thioorganique Macromoléculaire (LSMTM), Faculté de Chimie, Université des Sciences et de la Technologie Houari Boumediene, El Alia, BP 32, Bab Ezzouar, 16111, Algiers, Algeria, e-mail: bouslah_naima@yahoo.fr

Nesma Baa Belmessaoud and Nabila Haddadine: USTHB, Laboratoire de Synthèse Macromoléculaire et Thioorganique Macromoléculaire (LSMTM), Faculté de Chimie, Université des Sciences et de la Technologie Houari Boumediene, El Alia, BP 32, Bab Ezzouar, 16111, Algiers, Algeria

application [1–7]. These multi-functional systems, which are used to deliver drugs at certain rates, have been developed to overcome the limitations of conventional formulations. Conventional release dosage forms are known to provide an immediate release of the drug and thus produce a wide range of fluctuations in drug concentrations in the bloodstream, and may lead to under or over medication. Formulations that can enable the drug to be given once daily, as an example, are vital for improving patient compliance and therapeutic efficacy.

Montmorillonite (Mt) is by far the most well studied of the smectite clays for controlled release applications [8–10]. Its layered structure, cation exchange capacity and water sorption properties have proven that this clay is a versatile and useful material for modulating drug delivery. Indeed, this clay can be used to prepare biomedical composites in which the drug molecules are intercalated between the layers and can be released under proper conditions. Furthermore, the intercalation could improve the stability of the drug and protect its original biological function. The combination of drug-containing clays to biopolymers can provide polymer-based drug delivery systems with enhanced properties in comparison with polymers or clays alone, such as easy degradation, biocompatibility and tunable mechanical properties [11, 12]. Carboxymethylcellulose (CMC) is a biodegradable, biocompatible, nontoxic and available derivative of cellulose which is usually used in pharmaceutical applications. This anionic watersoluble polymer has already been used successfully for the development of controlled drug-delivery systems [13–15]. However, the use of this biopolymer in sustained release systems may require the combination to other polymers because of its high drug release retardant effect. For this purpose, poly(ethylene glycol) (PEG) may be an excellent candidate, since the ability of PEG to influence the pharmacokinetic properties of drugs and drug carriers has been well established for years [16, 17].

Ibuprofen (Ib) is an important non-steroidal anti-inflammatory drug that possesses analgesic and antipyretic activity used for relieving pain and fever, and reducing inflammation [18, 19]. Due its fast metabolism in the human body, the plasma half-life of Ib is between 1.9 h and 2.2 h, and it has to be administered more than five times per day to achieve the expected therapeutic effect [20, 21]. Furthermore, it exhibits poor solubility in water

which reduces its bioavailability [22]. Several studies showed that poorly water-soluble crystalline drugs dissolve more rapidly in their amorphous form [23]. The present paper deals with the intercalation of Ib molecules into the interlayers of Mt with the aim of reducing its crystallized fraction. In order to control the release of Ib in the intestinal environment, a sodium MtIb hybrid was compounded with PEG, CMC polymers and their blend. The biocomposites were characterized by X-ray diffraction (XRD), Fourier transform infrared (FTIR) spectroscopy, differential scanning calorimetry (DSC) and thermogravimetric analysis (TGA). Particular attention has been paid to the development of specific interactions within the developed systems and their effect on the drug release properties of these biocomposites.

2 Materials and methods

2.1 Materials

PEG (Mw=10,000 g mol⁻¹), sodium CMC ($M_w = 700,000$; Degree of substitution = 0.9) were purchased from Aldrich Chemical Company (St. Louis, MO, USA). Ib (purity 99%) was used as supplied by Sigma-Aldrich Co. (St. Louis, MO, USA). The chemical structures of the drug and polymers used are illustrated in Figure 1.

The clay used is an Mt-rich bentonite (Mostaganem, Algeria) provided by the national non-ferrous mining products and valuable substances ENOF (Algiers, Algeria), and analyzed by its central laboratory. This native clay contains SiO₂ (58.5%), Al₂O₂ (19.5%), Fe₃O₂ (2.8%), MnO (0.06%), CaO (2.5%) MgO (3.4%), Na₂O (2.1%), K₂O (2.2%), H₂O (7.1%), as determined by chemical analysis. The cation exchange capacity was determined to be about 76 meg/100 g by conductometric titration. It was treated according to a standard procedure [24].

In a first step, the raw clay was purified with several washings in de-ionized water. The submicron

fraction of the clay was separated by gravity sedimentation. In a second step, we treated the purified clay in an HCl (Sigma-Aldrich, St. Louis, MO, USA) acid solution (1 N) in order to activate it. The third stage of the change was to standardize the existing cations in the interlayer space of Mt, and the saturation of the clay with NaCl (Sigma-Aldrich, St. Louis, MO, USA) solution (0.1 N). The dispersion was reacted three times with NaCl solution, centrifuged, and washed with de-ionized water until free of chloride as tested by AgNO, (Sigma-Aldrich, St. Louis, MO, USA) solution. The clay recovered at the end of this step was sodium Mt.

K, HPO, and NaOH (Sigma-Aldrich, St. Louis, MO, USA) used for the preparation of phosphate buffer solution, pH 7.4, were analytical grade and used as received.

2.2 Drug loading

Some 4 g of Mt was dispersed in 100 ml of distilled water with vigorous stirring for 2 h at room temperature. The pH was adjusted to 13 with (0.1 M) NaOH. Then, 0.6 g of Ib was added and ultrasonically stirred at 70°C. After 2 h, the mixture was centrifuged at 3500 rpm for 30 min, and supernatant was filtrated to remove the floating small Mt particles. The Ib concentration in the supernatant was determined with an UV spectrophotometer at $\lambda_{max} = 264$ nm after dilution. The incorporation efficiency of MtIb was 13%.

2.3 Preparation of Mtlb/polymer composites

CMC, PEG and a CMC/PEG blend in a 50/50 weight ratio were dissolved in de-ionized water and stirred for 2 h to obtain homogeneous solutions. Some 0.4 g of MtIb hybrid was added to 0.1 g of each biopolymer or polymer blend solution and stirred for 3 h into an ultrasonic bath at 60°C to obtain homogeneous suspension. The mixture was then casted onto plates. After evaporation of most of the

Figure 1: Structural formula of (A) ibuprofen (2-(4-isobutylphenyl) propionic acid), (B) sodium salt carboxymethylcellulose (CMC), and (C) poly(ethylene glycol) (PEG).

solvent at room temperature, the samples were placed in a vacuum at 50°C. For the drug release study, the films were milled and then compressed to obtain 6 mm diameter tablets. The obtained samples were named MtIb/PEG, MtIb/CMC and MtIb/PEG-CMC.

2.4 Characterization

The amount of drug intercalated into Mt was calculated from the difference between the concentration of the solutions before and after intercalation, by UV spectroscopy and confirmed by TGA study.

XRD patterns were recorded at 4°/min on a Phillips PW1710 diffractometer by using CuKα radiation at a generator voltage of 50 kV and a generator current of 180 mA. All samples were examined in powder form.

FTIR spectra were recorded at room temperature with a Perkin Elmer FTIR Spectrum Two, using 32 scans and a resolution of 2 cm⁻¹, from 4000 cm⁻¹ to 400 cm⁻¹. The dry powdered samples were mixed with KBr (7% w/w).

TGA was performed on a TAQ 500 instrument under nitrogen atmosphere from room temperature to 600°C at a heating rate of 10°C/min.

The DSC study was carried out using a Perkin Elmer, DSC Diamond. Samples with weights between 5 mg and 10 mg were sealed into an aluminum pan. An empty aluminum sealed pan was used as reference material. The temperature was raised from 25°C to 180°C at a heating rate of 20°C/min under nitrogen atmosphere.

2.5 In vitro drug release experiments

The in vitro drug release behavior was carried out by placing the drug loaded samples of constant size and surface area in simulated intestinal fluid (phosphate buffer solution pH 7.4), in a water bath with stirring at a speed of 100 rpm at 37 ± 0.5 °C. Aliquots (5 ml) were withdrawn at periodic intervals and were immediately replaced by the same volume of fresh medium. The aliquots, after suitable dilution, were analyzed using the UVvisible Perkin Elmer lambda 20 spectrophotometer. The UV-visible absorbances of Ib solutions were measured at $\lambda_{\text{max}} = 264 \text{ nm}$. The release amount was calculated by a previously established calibration curve. The test was carried out in triplicate using the basket method. For comparative purposes, commercial 400 mg Ib tablets from Nadpharmadic Production (Algeria), containing corn starch, pregelatinized starch, sodium starch glycolate, stearic acid and aquapolish as excipients, were also tested.

3 Results and discussion

3.1 XRD study

XRD analysis was first used to evaluate the intercalation of the drug into the interlayer space of the Mt galleries. The XRD patterns of Ib, Mt and MtIb are shown in Figure 2A. The (001) reflection for pure Mt was observed at 7.06° corresponding to a d-spacing of 12.51 Å as calculated from Bragg's law. This peak shifted to lower angles at 5.56° upon adding Ib, suggesting that the d-spacing of Mt increased to 15.88 Å. The increased basal spacing after the introduction of Ib within Mt is evidence of the intercalation of Ib molecules into Mt galleries and confirmed the successful preparation of the intercalated MtIb hybrid. Pure Ib exhibited typical reflection at 20 6.16°, 12.21°, 16.61°, 19.00 and 22.30°. The disappearance of these peaks in the MtIb diffractogram revealed that the Ib incorporated in the clay sample was in the amorphous state [25]. This observation indicates that the clay platelets inhibit the crystallization of Ib as a consequence of the presence of good interactions between the drug and the clay.

A second XRD study was carried out to investigate the possibility of the intercalation of the polymer macromolecules into the drug loaded Mt galleries. In Figure 2B, the Mt peak for the (001) plane is shifted toward lower angles in MtIb /PEG than in the MtIb pattern, suggesting that the intercalation of the PEG macromolecules further increased the interlayer space in the clay layers. The same phenomenon was observed for the MtIb/ PEG-CMC diffractogram. The displacements to lower angles are reported in Table 1.

The CMC biopolymer displayed a common broad diffraction peak at $2\theta = 22.5^{\circ}$ illustrating the amorphous nature of CMC. In the case of the MtIb/CMC formulation, there was no peak observed in the diffraction pattern corresponding to the layered Mt clay. This phenomenon implied that Mt layers in the MtIb/CMC composites were exfoliated as a result of the presence of strong interactions between the clay and the carbohydrate polymer.

3.2 FTIR study

FTIR spectroscopy was first used to confirm the insertion of the Ib molecules within the Mt layers. FTIR spectra of Mt and MtIb are illustrated in Figure 3A. In the FTIR Mt spectrum, the broad band centered near 3446 cm⁻¹ is due to the -OH stretching mode of interlayer water. The bands at 3621 cm⁻¹ and 3696 cm⁻¹ are due to the -OH stretching mode of Al-OH and Si-OH of the Mt structure [26]. The

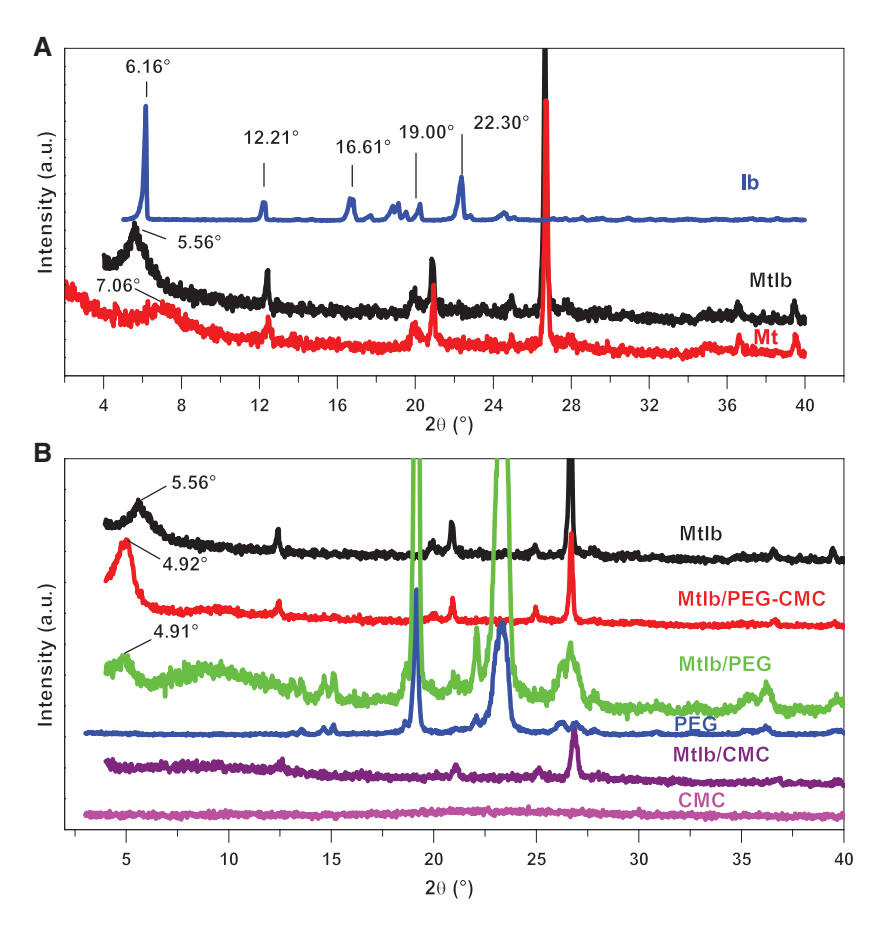


Figure 2: X-ray diffraction patterns of (A) ibuprofen (Ib), montmorillonite (Mt) and MtIb hybrid, (B) MtIb, poly(ethylene glycol) (PEG), carboxymethylcellulose (CMC), and MtIb/PEG, MtIb/CMC, MtIb/PEG-CMC composites.

Table 1: X-ray diffraction (XRD) data obtained for the biocomposites.

Composites	2θ (°)	d-spacing (Å)		
Mt	7.06	12.51		
Mtlb	5.56	15.88		
MtIb/PEG	4.91	17.91		
MtIb/CMC	_	_		
MtIb/PEG-CMC	4.92	17.90		

CMC, carboxymethylcellulose; Ib, ibuprofen; Mt, montmorillonite; PEG, poly(ethylene glycol).

absorption peak in the region of 1641 cm⁻¹ is attributed to the -OH bending mode of absorbed water. The Si-O and Al-O bonds are, respectively, observed at 1037 cm⁻¹ and 620 cm⁻¹, and the Mg-O bond is assigned to the band at 530 cm⁻¹. In the Ib spectrum, a strong absorption band at 1706 cm⁻¹ assigned to the acid carbonyl groups was observed. The bands between 3090 cm⁻¹ and 3000 cm⁻¹ were related to the Ib C-H aromatic ring. The bands between 3000 cm⁻¹ and 2800 cm⁻¹ were the alkyl stretching vibrations of Ib. All characteristic bands belonging to Mt and Ib appeared in the spectrum of the MtIb hybrid, especially the bands in the 3040-2877 cm⁻¹ region corresponding to -C-H stretching of Ib, indicating the good insertion of the drug molecules in the Mt galleries. Furthermore, the displacement of the carbonyl band of Ib from 1706 cm⁻¹ to lower temperatures revealed that Ib interacted strongly with the Mt layer. The appearance of new bands at 1617 cm⁻¹ (asymmetric stretching) and 1550 cm⁻¹ (symmetric stretching) indicated the presence of carboxylate ions arising from electrostatic interactions between the drug and Mt. Indeed, the negatively charged sites at the clay surface are capable of extracting the carboxylic proton of Ib (Figure 4). The presence of these interactions may improve the solubility and/or modify the profile of drug release [27]. The negative charge on the clay surface results from the substitution of silica cations (Si4+) by aluminum cations (Al³⁺) in the clay sheet structure. The FTIR spectra of PEG, CMC, PEG-CMC and the corresponding biocomposites MtIb/CMC, MtIb/PEG and MtIb/PEG-CMC are presented in Figure 3B. To better visualize the interactions developed in the different systems, the FTIR spectra

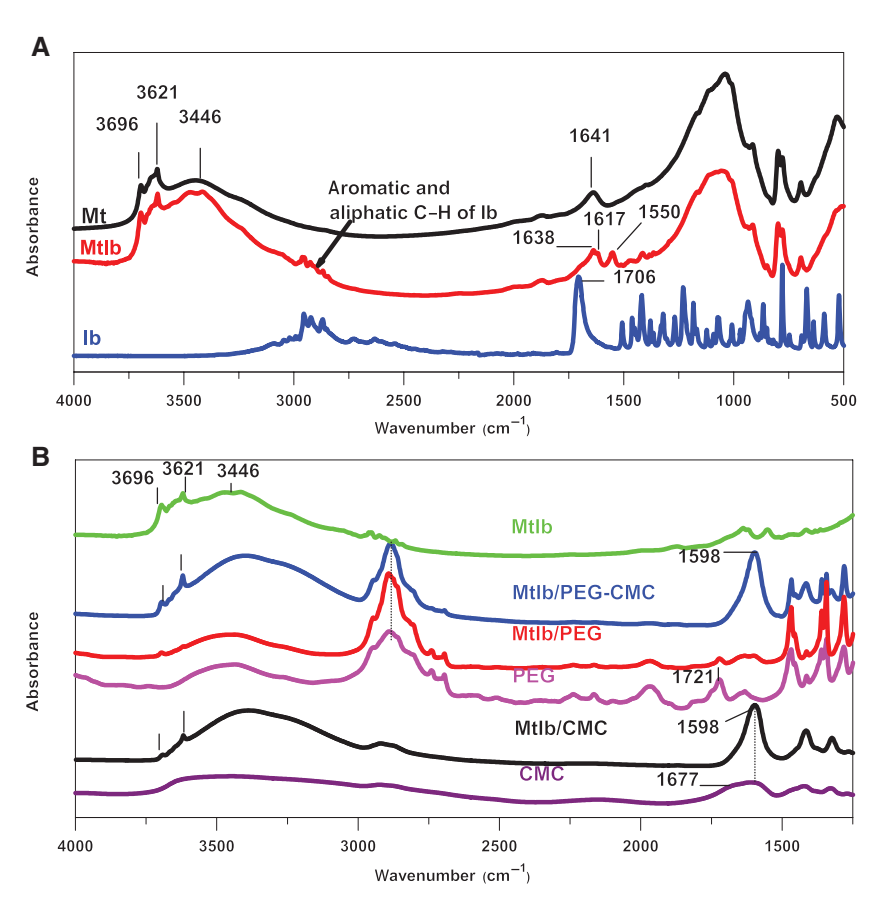


Figure 3: Fourier transform infrared (FTIR) spectra of (A) montmorillonite (Mt), ibuprofen (Ib) and MtIb hybrid, (B) MtIb, poly(ethylene glycol) (PEG), carboxymethylcellulose (CMC) and drug loaded composites.

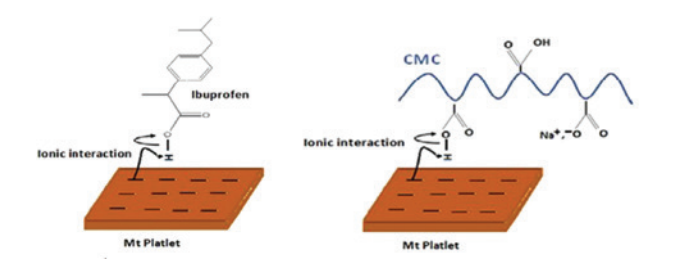


Figure 4: Illustration of clay/drug and clay/carboxymethylcellulose (CMC) interactions.

are displayed in the 4000–1250 cm⁻¹ region. In the MtIb/CMC, MtIb/PEG and MtIb/PEG-CMC composites spectra, the bands at 3696 cm⁻¹ and 3621 cm⁻¹ correspond to the stretching vibration of OH groups situated on the surface of the clay. In the CMC spectrum, a broad band with a double maximum at 1677 cm⁻¹ and 1598 cm⁻¹ corresponding to carboxylic and carboxylates (-COO⁻) groups, respectively, was observed. In the MtIb/CMC spectrum, this band becomes thinner and more symmetric with a maximum at 1598 cm⁻¹, suggesting that all carboxylic groups have been converted to carboxylate groups after their interaction

with the negatively charged clay surface (Figure 4). The MtIb/PEG-CMC spectrum showed a broad band at about 3423 cm⁻¹ corresponding to the O-H stretching groups of both PEG and CMC. The bands between 3000 cm⁻¹ and 2800 cm⁻¹ are the -CH alkyl stretching vibration of CMC, PEG and Ib [28]. The band of carboxylate groups which has been observed in the MtIb/CMC spectrum appeared at the same position in the MtIb/PEG-CMC spectrum, suggesting the same developed interaction between the CMC and the clay surface in the blend biocomposite.

3.3 DSC study

The DSC thermogram of Ib showed a melting endotherm at 83°C due to its crystalline structure (Figure 5). DSC thermograms of Mt and MtIb revealed very similar broad endotherms beginning at about 100°C, with maxima occurring at 130°C, indicative of loss of adsorbed and intercalated water from the clay particles. The endothermic peak due to the melting of Ib crystals was not observed in the MtIb hybrid spectrum. This observation is

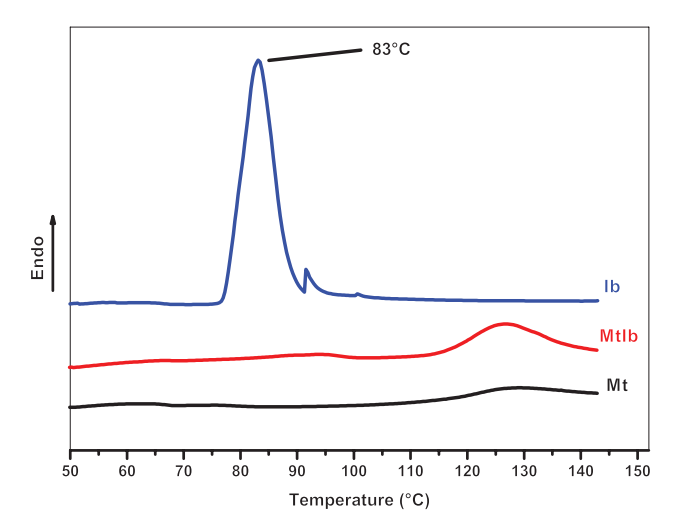


Figure 5: Differential scanning calorimetry (DSC) thermograms of ibuprofen (Ib), montmorillonite (Mt) and MtIb hybrid recorded on heating.

an indication of the amorphous state of the drug [29, 30] as already observed by XRD analysis, and confirms the development of specific interactions between the clay and the drug which hinder crystal growth.

The DSC thermogram for pristine PEG shows an endotherm at 70°C, which corresponds to its melting point. The melting endotherm has shifted slightly to lower temperatures at 68°C in the MtIb/PEG composite suggesting a less-ordered structure of PEG in the MtIb/PEG composite compared to its pure crystalline form Figure 6A. Furthermore, no peak corresponding to Ib was observed in the MtIb/PEG thermogram, confirming that the drug is still in its amorphous state in this composite. The PEG melting temperature decreased further after introduction of the CMC in the MtIb/PEG-CMC composite, which is an indication of the miscibility of PEG and CMC polymers [31]. Indeed, the decrease in the melting point in the blend composite is due to a decrease in PEG lamellar thickness as a result of polymer-polymer interactions.

The DSC thermograms of pristine PEG and MtIb/ PEG composites recorded upon cooling are illustrated in Figure 6B. The PEG thermogram showed an exothermic peak which corresponds to the crystallization temperature $T_c = 32^{\circ}$ C. The crystallization temperature of PEG in the MtIb/PEG composite was higher by 7°C than that of the neat PEG, suggesting that the clay hybrid MtIb has acted as a nucleating agent and enhanced the crystallization rate of PEG. In this case, in the molten state, the segments of the PEG molecules can easily interact with the surface of Mt, developing crystallization nuclei. This may be due to the high surface area of the nano-sized particles that enhanced heterogeneous crystallization. Similar results have been reported for nanocomposites by several authors [20, 21].

3.4 TGA

TGA was first used to prospect a possible delay in drug decomposition temperature because of drug intercalation in the clay interlayers. The thermal parameters used are

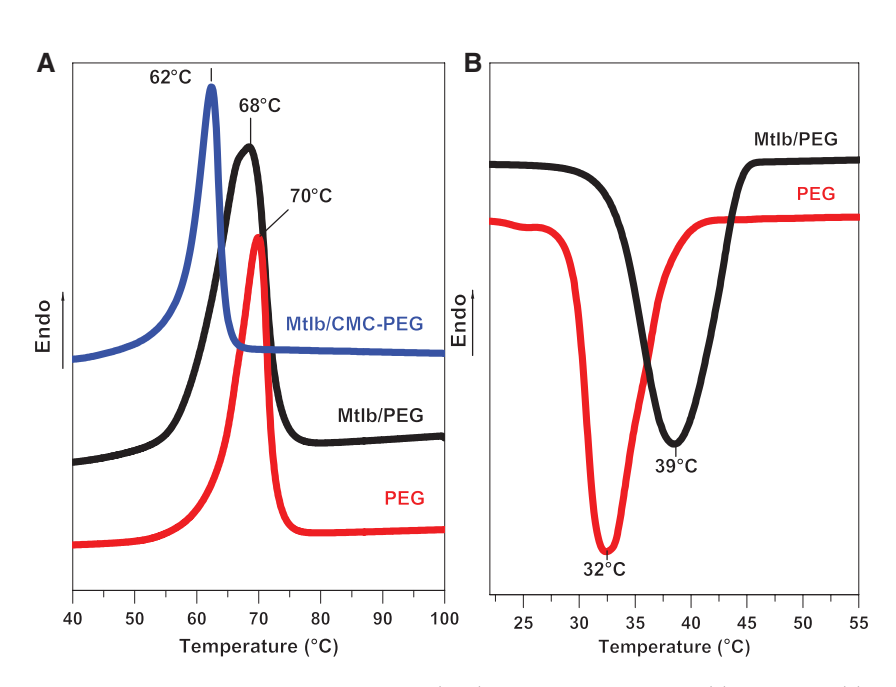


Figure 6: Differential scanning calorimetry (DSC) thermograms recorded (A) on heating (B) on cooling.

 T_{onset} and T_{max} . T_{onset} is defined as the temperature at which the weight loss just becomes detectable and Tmax as the temperature corresponding to maximum rate degradation. Figure 7A shows the TGA thermograms of Ib, Mt and MtIb. As can be seen, two major weight loss patterns were observed in the temperature range of 80-130°C and 450-750°C for Mt. The first weight loss corresponds to evaporation of adsorbed water. The second weight loss is due to the loss of structural hydroxyl groups of Mt [32]. The thermal degradation of pristine Ib begins at 114°C with a maximum weight loss at 225°C, as determined from the derivative curve. The MtIb hybrid showed a weight loss in the temperature region from 393°C to 516°C, corresponding to the degradation of the drug in clay galleries. This delay in drug decomposition suggests a thermal stabilization effect resulting from drug intercalation of the drug molecules in the interlayer spaces of the clay.

TGA analysis was also conducted on pure matrices PEG, CMC and PEG/CMC, and the MtIb loaded matrices MtIb/PEG, MtIb/CMC and MtIB/PEG-CMC. The results are presented in Figure 7B. PEG showed a single abrupt weight loss with a T_{max} located at 390°C corresponding to backbone chain scission, since PEG has a simple linear chain structure. The CMC thermogram revealed three weight loss regions, suggesting the coexistence of more than one degradation process. After moisture dehydration that starts just above room temperature, CMC showed a first chains degradation from 250°C to 315°C. A second

stage of decomposition with a decreased rate is observed from 315°C to 515°C. The residual mass after this stage was about 36% indicating that up to 600°C, the total decomposition of the polymer did not take place.

MtIb/PEG and MtIb/CMC thermograms exhibited higher thermal stability than the corresponding polymers PEG and CMC separately. Furthermore, the initial decomposition of both MtIb/PEG and MtIb/CMC occurs at 267°C. In the case of the MtIb/PEG-CMC nanocomposite, the onset temperature shifts to the high values compared to MtIb/PEG and MtIb/CMC nanocomposites. This enhancement in the thermal stability can be attributed to the miscibility of the PEG-CMC blend, which is the result of the development of specific interactions between PEG and CMC as already observed in the DSC study. The increase in the onset temperatures can be associated to the break of the specific interactions that exist in the miscible blend.

3.5 In vitro drug release study

The sustained release profiles of Ib in a phosphate buffer solution at pH 7.4, from the different drug delivery systems compared to a commercial tablet are shown in Figure 8.

The MtIb hybrid exhibited a burst effect with 80% release of Ib within 1 h. This is probably due to the repulsive ionic interactions occurring between two negatively charged species. Indeed, in the buffer solution at pH 7.4,

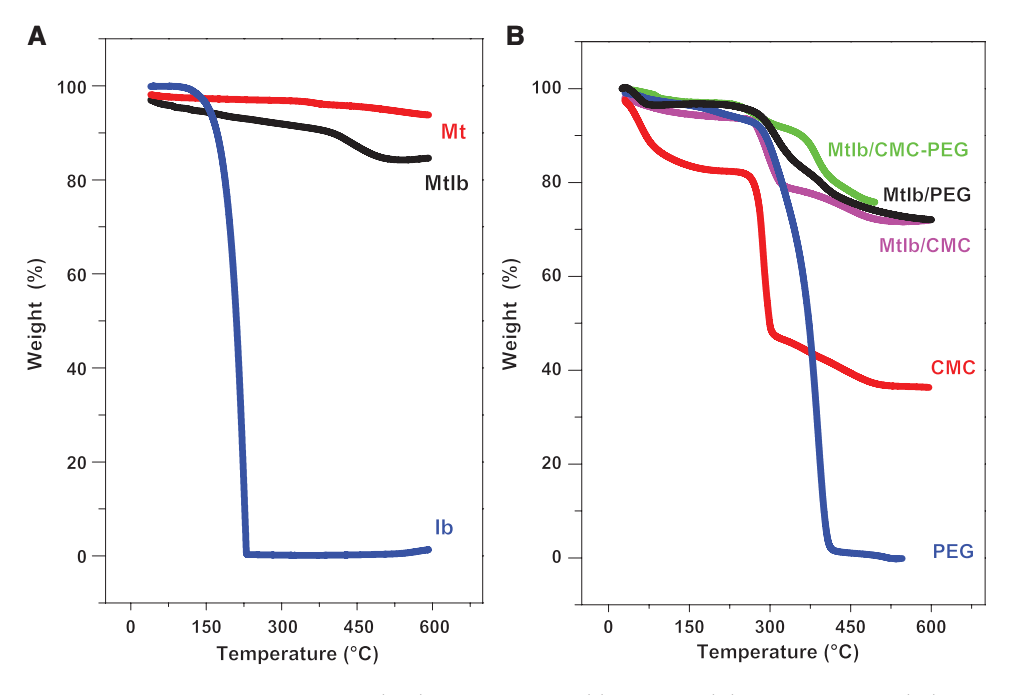


Figure 7: Thermogravimetric analysis (TGA) thermograms of (A) ibuprofen (Ib), montmorillonite (Mt) and Mtlb hybrid, (B) poly(ethylene glycol) (PEG), carboxymethylcellulose (CMC) and drug loaded composites.

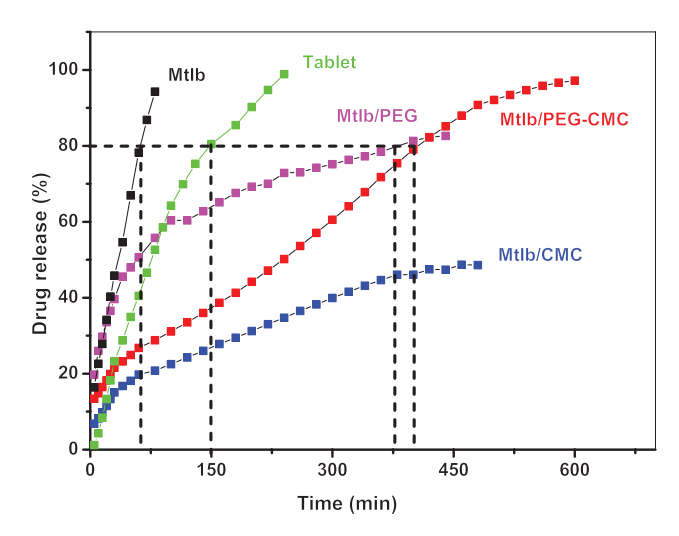


Figure 8: Release profiles in simulated intestinal fluid (pH 7.4) at 37 ± 0.5 °C.

the drug Ib (pKa=5.2) will be in the conjugate base form (-COO-). By contrast, the negative charge on the clay surface increases in this medium [33]. Therefore, the repulsion forces between the clay surface and the drug molecules are strong enough to speed up the drug release.

In comparison, the commercial tablet showed a more continuous release since 80% of the drug was delivered in about 2.5 h. This is probably attributed to the presence of excipients in the tablet. The release rate was greatly decreased after the introduction of PEG, CMC and the PEG-CMC polymer blend in the system in comparison to both the MtIb hybrid and the commercial tablet. For the MtIb/PEG system, a sustained release of 80% was reached after 6.2 h. The reduced drug release rate may be attributed to the resulting intercalated structure in the MtIb/PEG composite as illustrated in the XRD study. Such an intercalated structure may increase the diffusion path length of the drug towards the dissolution medium. However, the problem of the burst effect was not completely suppressed by the introduction of PEG in the system.

In the MtIb/CMC system, the release period was further prolonged. However, the total cumulative percentage of the drug released was only about 50%. This can be explained by the decrease in the mobility of the drug molecules induced by the exfoliated structure of the MtIb/ CMC composite. Furthermore, the presence of interactions between the Ib molecules and CMC macromolecular chains attached to the clay sheets, as illustrated in Figure 4, will prevent some drug molecules from being released.

The use of the MtIb/PEG-CMC system sustained the release of Ib more significantly, since 80% of the drug released was reached after 7 h. This can be explained by the presence of interactions between the carboxylic groups of the CMC and the PEG ether groups which will generate entanglement of the chains occupying a large space in the interfoliar space, thus delaying the release of the drug molecules. Furthermore, the phenomenon of burst effect has been totally avoided minimizing any initial toxicity associated with a high dose. An almost total release was obtained in 10 h.

3.6 Kinetics of drug release

To better understand the mechanism by which the drug release from the different carriers is governed, several kinetic models have been applied.

3.6.1 Zero-order model

This model describes systems where the drug release is only a function of time and the process takes place at a constant rate independent of drug concentration. This model can represent drug dissolution from dosage forms that do not disaggregate and release the drug slowly:

$$Q_t = Q_0 + k_0 t \tag{1}$$

where Q_t is the amount of drug dissolved at time t, Q_0 is the initial amount of drug in the solution and k_0 is the zero order release constant.

3.6.2 First-order model

$$ln Q_t = lnQ_0 - k_t t$$
(2)

where Q_t is the amount of drug released, Q_0 is the initial amount of drug and k_1 is the first order rate constant. This model describes the dissolution of water-soluble drugs from porous matrices.

3.6.3 Higuchi model [34, 35]

This model is the most often used to describe the release rate of both water soluble and poorly soluble drugs from a matrix system, usually a polymeric matrix, where the loading of the drug exceeds its solubility. This model is often applicable to the different geometrics and porous system:

$$Q_t = k_H t^{1/2} \tag{3}$$

where Q_t is the amount of drug released on time t and k_H is the release constant of Higuchi.

Table 2: Drug release kinetic parameters from the various biocomposites.

Formulation	,	Zero order		First order		Higuchi		Korsmeyer-Peppas		
	R ²	k _o	R ²		R ²	K _H	R ²	K _P	n	
MtIb/PEG	0.96	1.42	0.88	24.31	0.99	6.43	0.98	15.02	0.34	
Mtlb/CMC	0.97	1.21	0.83	15.11	0.99	2.70	0.98	4.02	0.43	
MtIb/PEG-CMC	0.98	1.31	0.90	19.41	0.99	3.16	0.98	9.5	0.30	

CMC, carboxymethylcellulose; Ib, ibuprofen; Mt, montmorillonite; PEG, poly(ethylene glycol).

3.6.4 Korsmeyer-Peppas model [36, 37]

Korsmeyer et al. [36] derived a simple relationship, which describes the release of drug from a polymeric system. To illustrate the mechanism of drug release, first 60% of drug release data was fitted to Eq. (4):

$$\frac{Q_t}{Q_{\infty}} = k_{\text{KP}} t^n \tag{2}$$

where $\frac{Q_{_{t}}}{Q_{_{-}}}$ the fraction of drug released at time t, $k_{_{\mathrm{KP}}}$ is the rate constant and "n" is the release exponent. In this model, the value of "n" characterizes the release mechanism of the drug.

In the Fickian model (Case I), n = 0.5, the drug release is governed by diffusion. The solvent transport rate or diffusion is much greater than the process of polymeric chain relaxation.

When 0.5 < n < 1, the model is non-Fickian or anomalous transport, and the mechanism of drug release is governed by diffusion and swelling or relaxation of polymeric chains. When n=1, the model is non-Fickian, Case II (relaxational transport), the drug release rate corresponds to zero-order release kinetics and the mechanism driving the drug release is the relaxation of polymeric chains.

The correlation coefficient R² values were determined for evaluation of accuracy and prediction ability of these models. The values of correlation coefficient (R2) and rate constant (k) for the different kinetic models are reported in Table 2.

The best fit was obtained for the Higuchi release model: the Ib release rate was proportional to the square root of time. The lowest $K_{_{\!\!\!H}}$ constant was obtained for MtIb/CMC, which corresponded to the lowest release rate of Ib among the prepared polymeric matrices. Furthermore, the rate constants obtained according to this model are decreasing in the order MtIb/PEG > MtIb/ PEG-CMC > MtIb/CMC, indicating that an adjustment of the kinetic release may be obtained by tailoring the blend composition in the matrix.

4 Conclusion

In this study, composites, based on clay and single polymers or a polymer blend, have been developed with promising benefits as drug carriers of Ib. XRD patterns of the MtIb hybrid showed an increase in the d-spacing, conforming the intercalation of Ib into the interlayer of Mt. No Ib characteristic XRD peak was observed in the case of the MtIb hybrid, nor an endothermic peak in the DSC thermogram corresponding to the melting of Ib, indicating the amorphous state of the drug in the MtIb hybrid. Changes in the FTIR spectra such as shift of the carbonyl band of Ib and appearance of new bands in the Mt-Ib hybrid spectrum are attributed to the physical interactions which are responsible for the amorphization of Ib in the biocomposites. The DSC study revealed the competing effects of the Mt acting as a nucleating agent whilst altering the crystallization behavior of PEG by inhibiting chain folding. All Mt-Ib formulations containing neat PEG, neat CMC, and the PEG-CMC blend resulted in a sustained release of Ib. The particular potential of the polymer blend in the control of the burst release, as well as the rate and amount of drug released, have been highlighted. In this composite, the presence of both polymer/clay and polymer/polymer interactions has enhanced the controlled drug release properties in biological media.

References

- [1] Abdeen R, Salahuddin N. J. Chem. 2013, 2013, 1-9.
- [2] Kianfar F, Dempster NM, Gastell E, Roberts M, Hutcheon GA. J. Nov. Drug Res. 2017, 1, 1-9.
- [3] Sandri G, Bonferoni MC, Ferrari F, Rossi S, Aguzzi C, Mori M, Grisoli P, Cerezo P, Tenci M, Viseras C, Caramella C. Carbohydr. Polym. 2014, 102, 970-977.
- [4] Onnainty R, Granero G. Nanomed. Nanotechnol. J. 2017, 1, 114.
- [5] Bee SL, Abdullah MAA, Bee ST, Sin LT, Rahmat AR. Prog. Polym. *Sci.* 2018, 85, 57–82.
- [6] Anirudhan TS, Gopal SS, Sandeep S. Appl. Clay. Sci. 2014, 88-89, 151-158.
- [7] Guo F, Aryana S, Han Y, Jiao Y. Appl. Sci. 2018, 8, 1696.

- [8] Viseras C, Carazo E, Borrego-Sanchez A, García-Villén F, Sánchez-Espejo R, Cerezo P, Aguzzi C. Clays Clay Miner. 2019, 67, 59-71.
- [9] Michael G, Ammit J, Gu A, Wheate JN. Inorg. Chim. Acta. 2014, 421, 513-518.
- [10] Mousavi S, Hashemi SA, Salahi S, Hosseini M, Amani AM, Babapoor A. Curr. Top. Util. Clay. Ind. Med. Appl. 2018, 9, 167-191.
- [11] Kevadiva BD, Joshi GV, Mody HM, Bajaj HC. Appl. Clay. Sci. 2011, 52, 364-367.
- [12] Hitzky ER, Darder M, Fernandes FM, Wicklein B, Alcantara ACS, Aranda P. Prog. Polym. Sci. 2013, 38, 1392-1414.
- [13] De Oliveira RL, Da Silva Barud H, De Salvi DTB, Perroti GF, Ribeira SJL, Constantino VRL. Ind. Crops. Prod. 2015, 69, 415-423.
- [14] Mahdavinia G, Afzali A, Etemadi H, Hosseinzadeh H. Nanomed. Res. J. 2017, 2, 111-122.
- [15] Barkhordari S, Yadollahi M, Namazi H. J. Polym. Res. 2014, 21, 454-462.
- [16] Zhao Y, Zou M, Liao H, Du F, Lei F, Tan X, Zhang J, Huang Q, Zhou J. Polymers 2019, 11, 1684.
- [17] Knop K, Hoogenboom R, Fischer D, Schubert US. Chem. Int. Ed. 2010, 49, 6288-6308.
- [18] Rao YF, Xue D, Pan H, Feng J, Li Y. Chem. Eng. J. 2016, 283, 65-75.
- [19] Rehman F, Rahim A, Airoldi C, Volpe PLO. Mater. Sci. Eng., C. 2016, 59, 970-979.
- [20] Ibuprofen. The International Encyclopedia of Adverse Drug Reactions and Interactions, 2016, 5-12.
- [21] Bédouet L, Moine L, Pascale F, Nguyen VN, Labarre D, Laurent A. Int. J. Pharm. 2014, 459, 51-61.

- [22] Nokhodchi A, Amire O, Jelvehgari M. Daru. 2010, 18, 74-83.
- [23] Botana A, Mollo M, Eisenberg P, Sanche RMT. Appl. Clay Sci. 2010, 47, 263.
- [24] Kevadiya BD, Joshi JV, Bajaj HC. Int. J. Pharm. 2010, 388, 280-286.
- [25] Pattnaik S, Swain K, Rao JV, Talla V, Prusty KB, Subudhi K. RSC Adv. 2015, 5, 74720-74725.
- [26] Arslan M, Tasdelen MA, Uyar U, Yagci Y. Eur. Polym. J. 2015, 71, 259-267.
- [27] De Sousa Rodrigues LA, Figueiras A, Veiga F, Freitas R, Nunes LCC, Da Silva Filho EC, Da Silva Leite CM. Colloids Surf., B 2013, 103, 642-651.
- [28] El-Houssiny AS, Ward AA, Mostafa DM, Abd-El-Messieh SL, Abdel-Nour KN, Darwish MM, Khalil WA. Adv. Nat. Sci.: Nanosci. Nanotechnol. 2016, 7, 025014.
- [29] Bounabi L, Bouslah Mokhnachi N, Haddadine N, Ouazib F, Barille R. J. Drug Delivery Sci. Technol. 2016, 33, 58-65.
- [30] Kong Y, Ma Y, Lei L, Wang X, Wang H. Polymers 2017, 9, 42.
- [31] Kevadiya BD, Joshi GV, Mody HM, Bajaj HC. Appl. Clay Sci. 2011, 52, 364-367.
- [32] Zheng JP, Luan L, Wang HY, Xi LF, Yao KD. Appl. Clay Sci. 2007, 36, 297-301.
- [33] Kevadiya BD, Patel TA, Jhala DD, Thumbar RP, Brahmbhatt H, Pandya MP, Rajkumar S, Jena PK, Joshi GV, Gadhia PK, Tripathi CB, Bajaj HC. Eur. J. Pharm. Biopharm. 2012, 81, 91-101.
- [34] Higuchi T. J. Pharm. Sci. 1963, 84, 1145-1149.
- [35] Siepmann J, Peppas NA. Int. J. Pharm. 2011, 418, 6-12.
- [36] Korsmeyer RW, Gurny R, Doelker E, Buri P, Peppas NA. Int. J. Pharm. 1983, 15, 25-35.
- [37] Korsmeyer R, Peppas NA. J. Membr. Sci. 1981, 9, 211-227.